Electronic Supplementary Material (ESI) for Journal of Materials Chemistry A.

Supporting Information

Highly Ionic Conductive, Self-healable Solid Polymer Electrolyte Based on Reversibly Interlocked Macromolecule Networks for Lithium Metal Batteries Workable at Room Temperature

Zi Xin Huang[a†], Zhen Hua Xie[a,b,c†], Ze Ping Zhang[a*], Ting Zhang[a], Min Zhi Rong[a*], and Ming Qiu Zhang[a*]

[a] Key Laboratory for Polymeric Composite and Functional Materials of Ministry of Education, GD HPPC Lab, School of Chemistry, Sun Yat-Sen University, Guangzhou 510275, P. R. China

[b] Institute of High Energy Physics, Chinese Academy of Sciences (CAS), Beijing 100049, P. R. China

[c] Spallation Neutron Source Science Center, Dongguan 523803, P. R. China

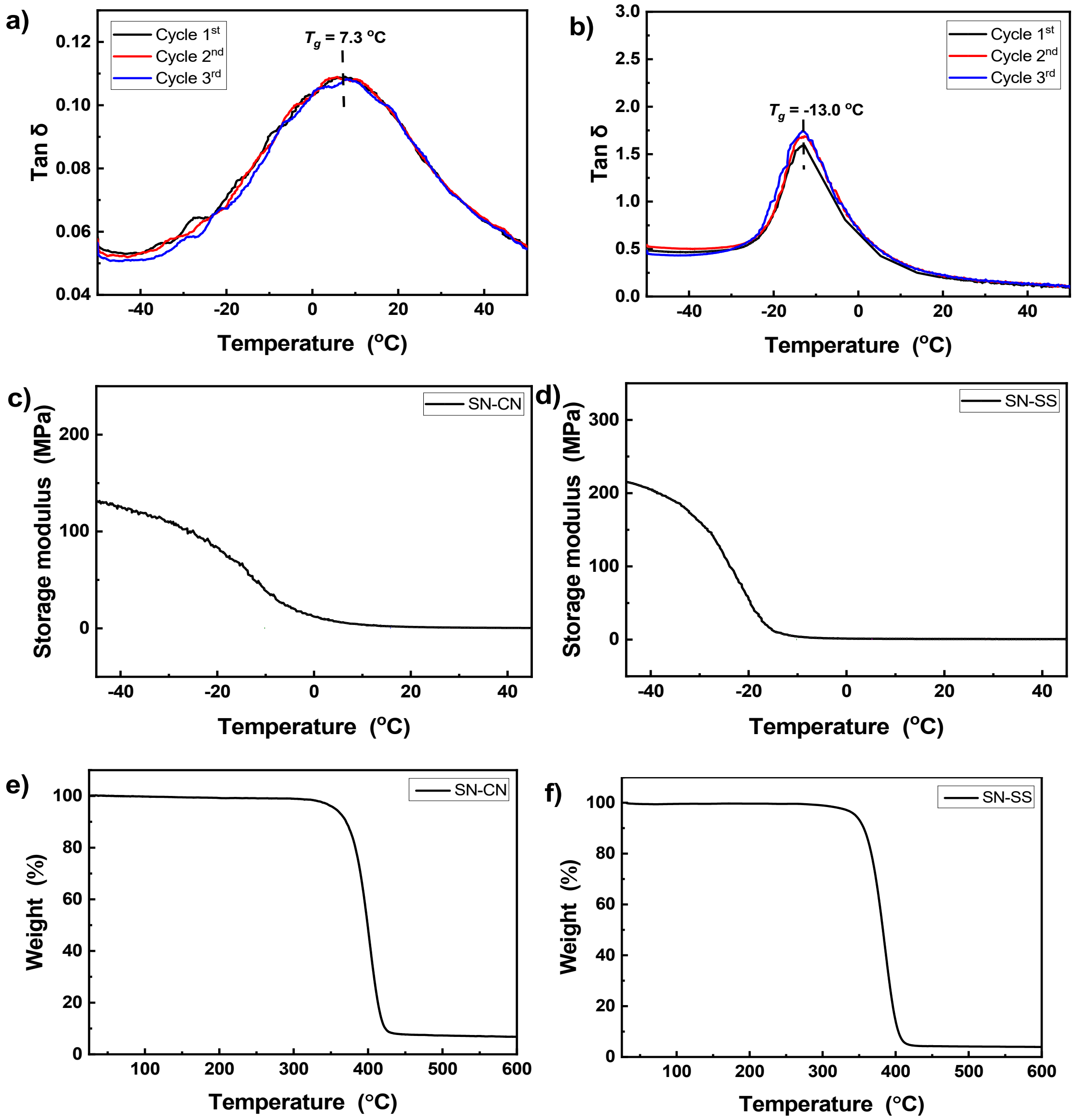

Fig. S1. Temperature dependence of tan δ and storage modulus of (a, c) SN-CN and (b, d) SN-SS measured at 1 Hz. TGA curves of (e) SN-CN and (f) SN-SS.

Table S1. Characterization of the SN-CN and SN-SS using DMA

Sample	ρ (g cm^{-3})	T_g (°C)	M_c[a] (g mol^{-1})
SN-CN	1.047	7.3	4821
SN-SS	1.169	−13.0	4548

[a] Molecular weight between crosslinks (M_c) of polymer was calculated from:

$$M_c = \frac{3(1-\frac{2}{\phi})\rho RT}{E'} \qquad \text{(S1)}$$

where ϕ is functionality of crosslinking site, ρ density, R the universal gas constant, T absolute temperature, and E' storage modulus at rubbery plateau zone, respectively. In this work, E' values at $T = T_g + 30$ °C were used for the calculation.

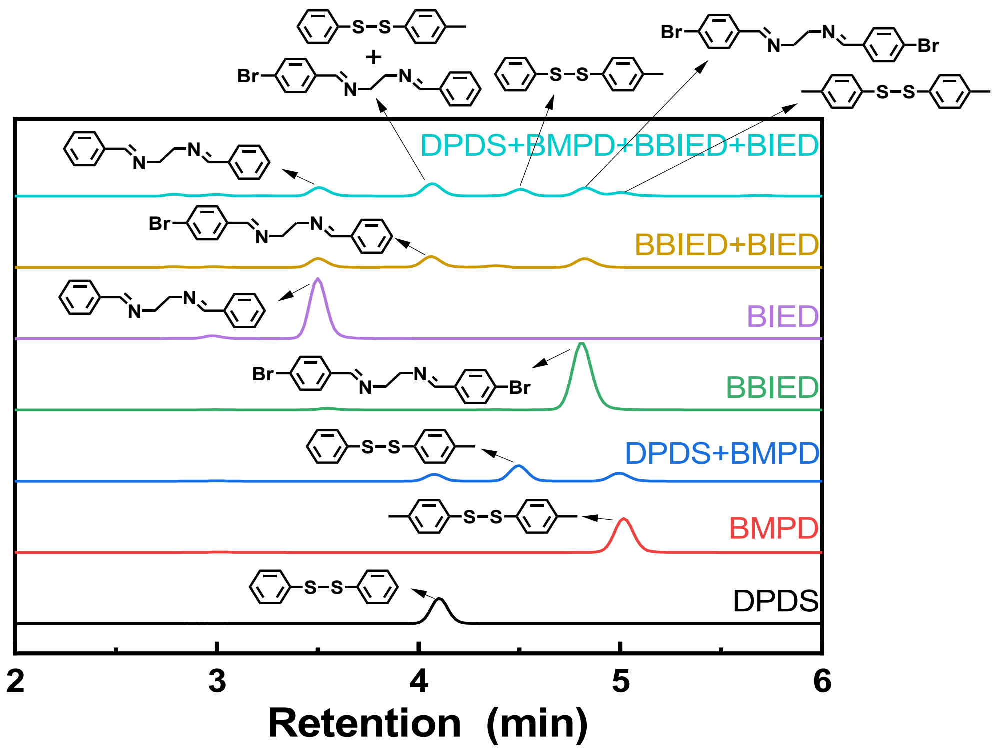

Fig. S2. HPLC curves of the model small molecules and their mixtures after exchange at room temperature for 2 h.

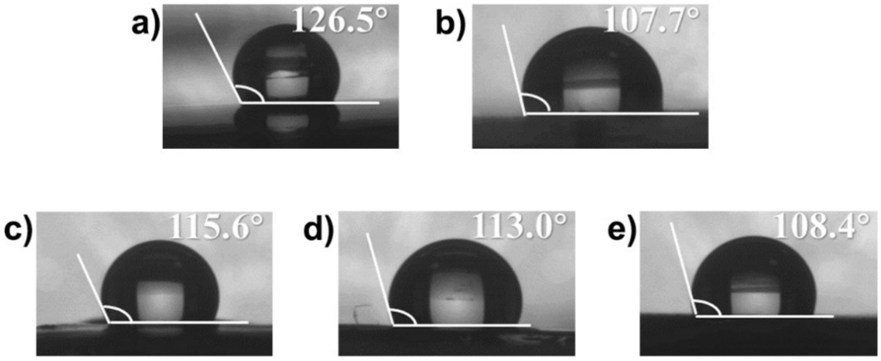

Fig. S3. Representative images of the water contact angles of (a) SN-CN-$LiPF_6$, (b) SN-SS-$LiPF_6$, (c) RILNs-3/1-$LiPF_6$, (d) RILNs-1/1-$LiPF_6$ and (e) RILNs-1/3-$LiPF_6$.

Table S2. Water contact angles and surface energies of the SPEs

Sample	Contact angle (°)	γ_s (mJ m^{-2})	γ_s^d (mJ m^{-2})	γ_s^p (mJ m^{-2})
SN-CN-$LiPF_6$	126.5	4.16	3.38	0.79
RILNs-3/1-$LiPF_6$	115.6	26.04	25.95	0.10
RILNs-1/1-$LiPF_6$	113.0	29.21	29.15	0.06
RILNs-1/3-$LiPF_6$	108.4	32.32	32.31	0.01
SN-SS-$LiPF_6$	107.7	33.04	33.03	0.01

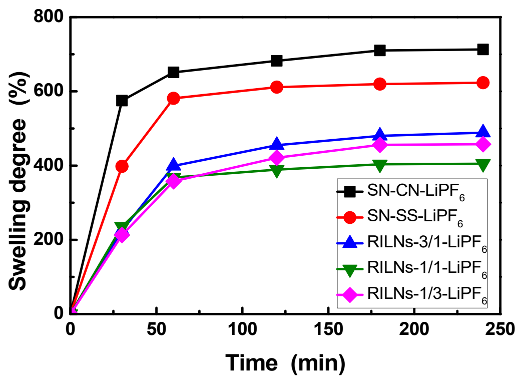

Fig. S4. Swelling degree as a function of time of the SPEs respectively based on the single networks and RILNs.

Table S3. Characterization of the SPEs using DSC and DMA

Sample	T_m (°C)	ΔH_f (J g^{-1})	X_c (%)	T_g (ºC)
SN-CN-$LiPF_6$	31.8	59.41	33.61	−7.1
RILNs-3/1-$LiPF_6$	N/A	N/A	N/A	−9.8
RILNs-1/1-$LiPF_6$	N/A	N/A	N/A	−13.1
RILNs-1/3-$LiPF_6$	N/A	N/A	N/A	−16.1
SN-SS-$LiPF_6$	45.2	63.18	35.74	−16.9

Table S4. Tensile properties of the SPEs

Sample	Tensile Strength (MPa)	Elongation at break (%)
SN-CN-$LiPF_6$	0.10±0.005	218.2±5.4
RILNs-3/1-$LiPF_6$	0.46±0.009	285.8±6.1
RILNs-1/1-$LiPF_6$	0.87±0.023	248.1±7.4
RILNs-1/3-$LiPF_6$	0.51±0.012	128.3±4.2
SN-SS-$LiPF_6$	0.32±0.007	98.5±4.0

Table S5. Ionic conductivities of the SPEs

Temperature (°C)	Ionic conductivity (10^{-4} S cm^{-1})				
	SN-CN-$LiPF_6$	RILNs-3/1-$LiPF_6$	RILNs-1/1-$LiPF_6$	RILNs-1/3-$LiPF_6$	SN-SS-$LiPF_6$
25	0.44	6.97	6.39	5.95	0.21
30	2.03	8.41	7.90	7.05	0.34
40	12.77	12.3	11.56	10.31	2.81
50	18.22	17.5	16.44	15.08	11.47
60	25.74	25.00	22.29	20.95	16.23
70	37.13	34.10	32.04	28.58	25.28

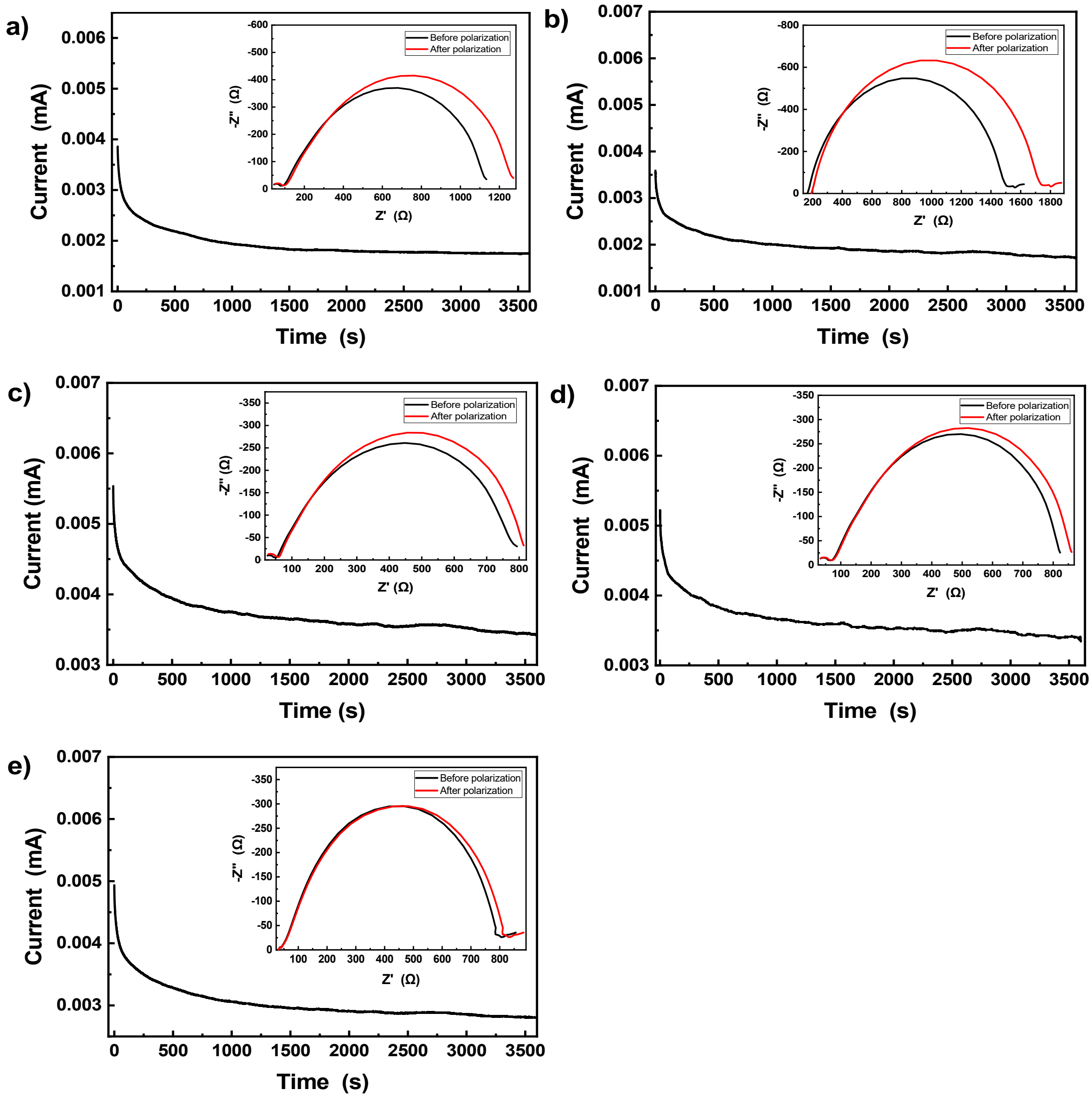

Fig. S5. Chronoamperometry profiles of the symmetric Li|SPE|Li cells with a polarization potential of 10 mV on the basis of (a) SN-CN-$LiPF_6$, (b) SN-SS-$LiPF_6$, (c) RILNs-3/1-$LiPF_6$, (d) RILNs-1/1-$LiPF_6$ and (e) RILNs-1/3-$LiPF_6$. The insets show the AC impedance spectra before and after polarization at 25 °C.

Table S6. Lithium-ion transference number of the SPEs calculated from **Fig. S5**

Sample	I_0 (mA)	I_s (mA)	R_0 (Ω)	R_s (Ω)	t_{Li^+}
SN-CN-$LiPF_6$	0.00386	0.00175	1134	1273	0.33
RILNs-3/1-$LiPF_6$	0.00553	0.00342	793	814	0.48
RILNs-1/1-$LiPF_6$	0.00517	0.00301	823	861	0.45
RILNs-1/3-$LiPF_6$	0.00493	0.00280	806	831	0.43
SN-SS-$LiPF_6$	0.00359	0.00169	1568	1806	0.30

Note: I_0, initial current; I_s, steady-state current; R_0, interfacial resistance before polarization; R_s, interfacial resistance after polarization.

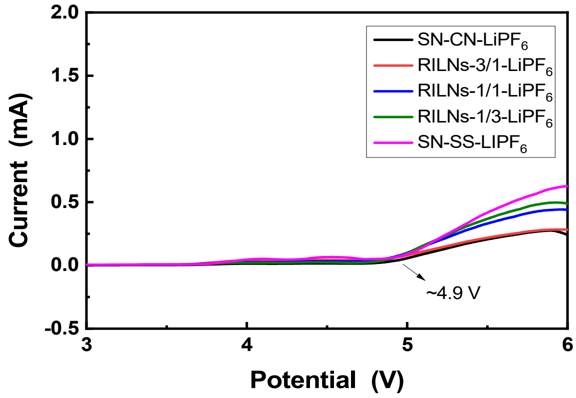

Fig. S6. LSV curves of the SPEs at 25 °C.

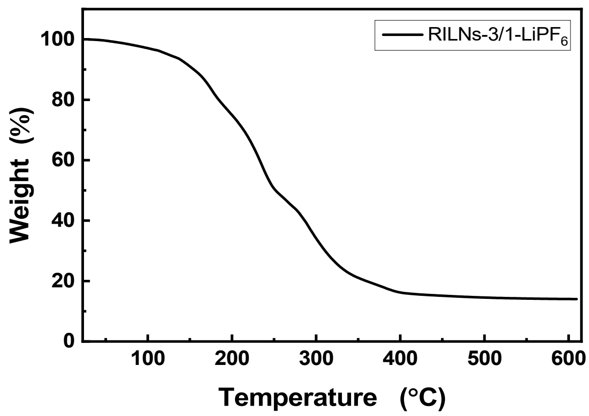

Fig. S7. The thermogravimetric curve of RILNs-3/1-$LiPF_6$.

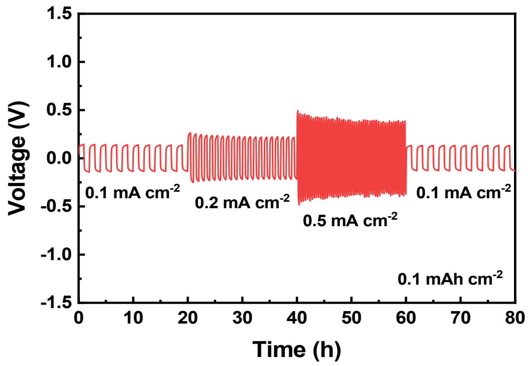

Fig. S8. Rate capability of the symmetric Li|RILNs-3/1-$LiPF_6$|Li cell at 25 °C. The capacity was fixed at 0.1 mAh cm^{-2}.

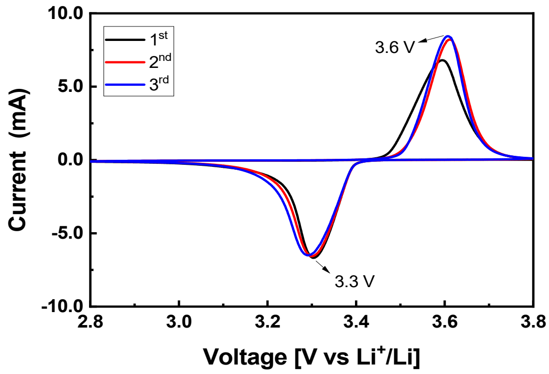

Fig. S9. CV curves of the Li|RILNs-3/1-$LiPF_6$|$LiFePO_4$ cell measured at a scan rate of 0.1 mV s^{-1}.

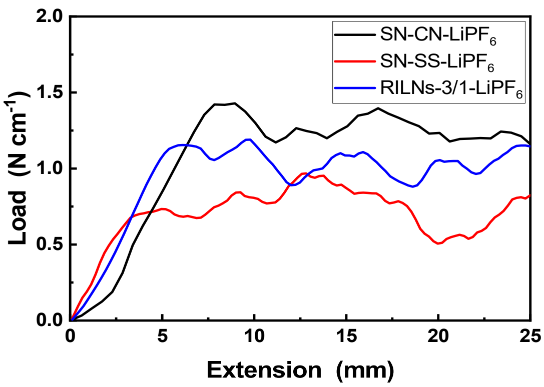

Fig. S10. Peel tests of the adhesion between the SPEs and lithium metal.

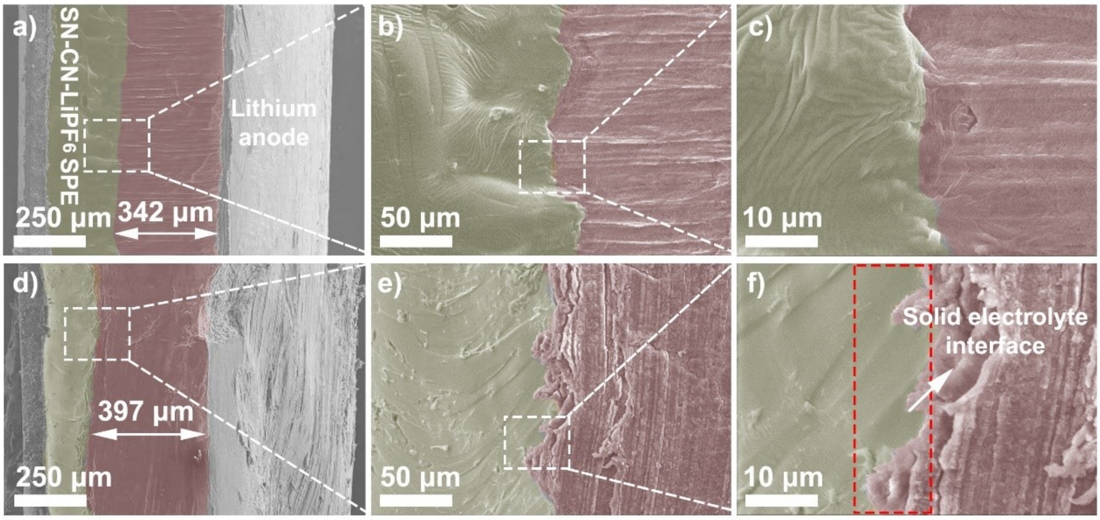

Fig. S11. SEM images of the cross-sections of Li|SN-CN-$LiPF_6$ (a, b, c) before and (d, e, f) after 50 cycles at 0.1 C. Note: The portions colored by light auburn denote the Li anode.

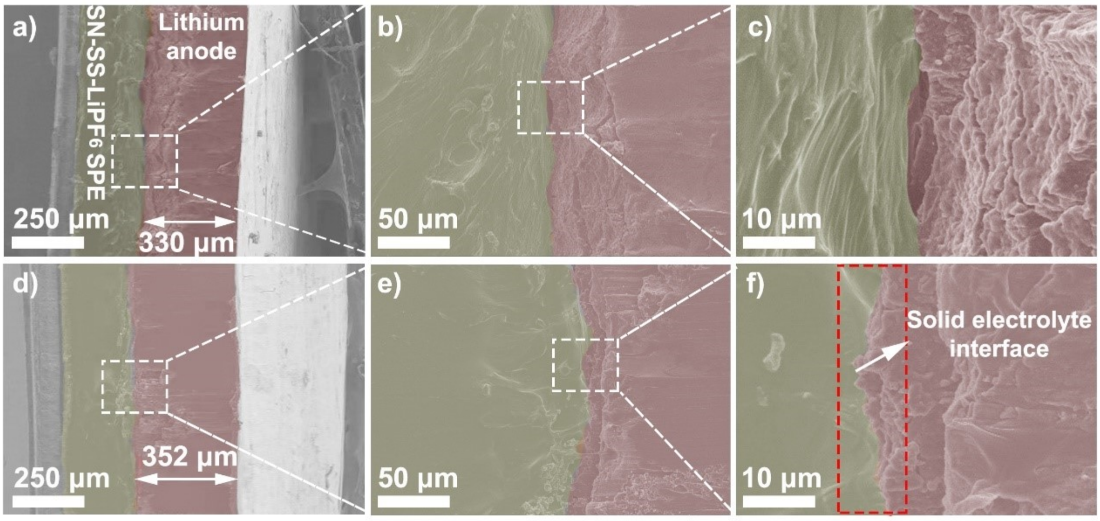

Fig. S12. SEM images of the cross-sections of Li|SN-SS-$LiPF_6$ (a, b, c) before and (d, e, f) after 50 cycles at 0.1 C. Note: The portions colored by light auburn denote the Li anode.

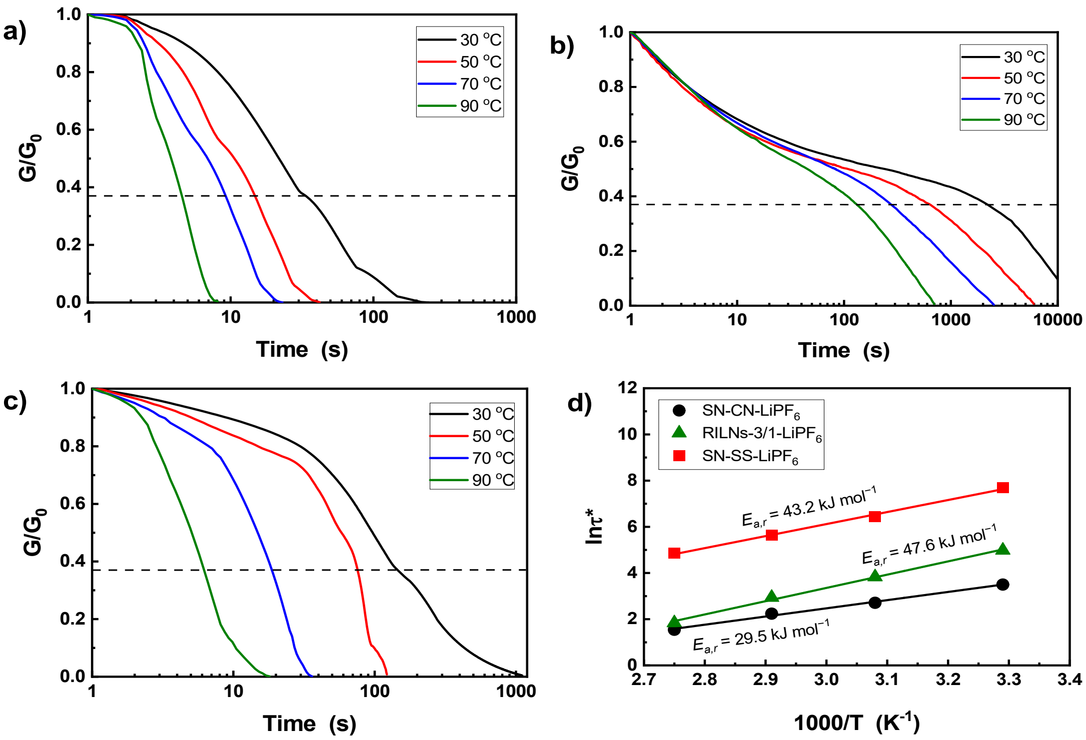

Fig. S13. Normalized stress relaxation of (a) SN-CN-LiPF$_6$, (b) SN-SS-LiPF$_6$, (c) RILNs-3/1-LiPF$_6$ as a function of temperature. (d) Fitting of the temperature dependences of the characteristic relaxation time, τ*, obtained from (a), (b) and (c) according to the Arrhenius equation.

Table S7. τ^* and $E_{a,r}$ of the SPEs obtained from **Fig. S13**

Sample	τ^* (s)				$E_{a,r}$
	90 °C	70 °C	50 °C	30 °C	(kJ mol^{-1})
SN-CN-LiPF$_6$	4.65	9.42	15.06	32.82	29.5
RILNs-3/1-LiPF$_6$	6.29	18.92	46.06	144.98	47.6
SN-SS-LiPF$_6$	130.11	280.18	626.37	2186.41	43.2

Table S8. Tensile properties and ionic conductivities of the original and healed RILNs-

3/1-$LiPF_6$

Samples name	Tensile strength（MPa）	Elongation at break (%)	Ionic conductivity at 25 °C (10^{-4} S cm^{-1})	Healing efficiency[a] (%)	Healing efficiency[b] (%)
Virgin	0.46	285.5	6.97	N/A	N/A
1st healed	0.43	269.9	6.51	94.5	93.4
2nd healed	0.40	261.8	6.09	91.7	87.4
3rd healed	0.34	238.0	5.90	83.4	84.6

[a] Calculated from the ratio of elongation at break of the healed specimen to that of the virgin specimen

[b] Calculated from the ratio of ionic conductivity of the healed specimen to that of the virgin specimen